



Design, Synthesis, ADMET Prediction and Docking Studies of Novel Aryl and Heteroaryl Chalcones as CDK2 Inhibitors

Fathimathul Farisha K, Rushdiya KK, Shahana K, Priyanka S*, Sangeetha S, Adithya G, Haripriya S, Baskar L

Department of pharmaceutical Chemistry, Grace College of Pharmacy, Kodunthirapully, Palakkad-670004, Kerala, India

Received: 27 December 2025

Revised: 10 January 2026

Accepted: 29 January 2026

ABSTRACT

Cyclin-dependent kinase 2 (CDK2) is a crucial therapeutic substrate in cancer treatment. The current study used in silico methods to develop, manufacture, and assess innovative aryl and heteroaryl chalcone derivatives for potential CDK2 inhibitory activity. Chemical structures were designed using ACD/ChemSketch. SwissADME, pkCSM, Lipinski's rule of 5 and PROTOX 3.0 were employed to estimate drug-likeness, pharmacokinetic characteristics, and ADMET scores. PyRx were used to conduct molecular docking studies against the CDK2 protein, such as 2FVD (Anticancer activity), 1MWT (Antibacterial activity), 4JK4 (Antioxidant activity) and 4O2B (Anthelmintic activity). The RCSB Protein Data Bank (PDB) provided the target proteins' three-dimensional crystal structures. The BIOVIA Discovery Studio Visualizer was used for both protein production and visualization. Several chalcone derivatives showed favorable binding energies and acceptable ADMET properties, suggesting their capability as prospective CDK2 inhibitors in further cancer-related drug discovery.

Keywords: Chalcones; Cyclin-dependent kinase-2 (CDK2); Molecular docking; ADMET prediction; In silico studies; Anticancer activity; Antibacterial activity; Antioxidant activity; Anthelmintic activity.

1. INTRODUCTION

The serine/threonine protein kinase known as cyclin-dependent kinase 2 (CDK2) interacts with cyclins E and A to regulate the progression of the cell cycle, especially during the change from G to S phase.^[1,2] Dysregulation of CDK2 activity has been implicated in uncontrollable cell growth, genetic instability, and tumorigenesis in a variety of malignancies like colorectal, breast, ovarian, and pulmonary tumors.^[3-5] Several small-molecule CDK2 inhibitors have demonstrated promising anticancer activity; however, limitations related to toxicity, resistance, and suboptimal ADME profiles have restricted their clinical translation.^[6,7]

Chalcones are distinguished by the occurrence of an α , β -unsaturated carbonyl bond between two aromatic ring structures, are privileged scaffolds in medicinal chemistry and have garnered a lot of interest because of their various pharmacological actions, notably anticancer, anti-inflammatory, and kinase inhibitory properties.^[8,9] The structural simplicity and synthetic accessibility of chalcones allow extensive structural modification, particularly through aryl and heteroaryl substitutions, facilitating structure-activity relationship studies (Fig. 1.0).^[10] Several chalcone-based derivatives have been reported to inhibit kinases involved in cell-cycle regulation, including CDK2, by interacting with key residues within the ATP-binding site.^[11-13]



Fig. 1: Basic structure of aryl and heteroaryl chalcones.



In recent years, computational approaches such as molecular docking and in silico ADMET prediction have become indispensable tools in the initial phases of drug development, allowing successful screening of scaffolds prior to synthesis and biological evaluation.^[14,15] These techniques lower experimental costs and speed up lead optimization by offering useful details on protein–ligand interactions, affinity for binding, and pharmacokinetic behaviour.^[16] To assess their potential as CDK2 inhibitors, the current study first designs and synthesizes novel aryl and heteroaryl chalcone derivatives, then moves on to ADMET prediction and docking experiments.

2. MATERIALS AND METHODS

2.1. Materials

We got 2-acetylthiophene, para-hydroxyacetophenone, 4-dimethylaminobenzaldehyde, cinnamaldehyde, ethanol, potassium hydroxide from Hemedia Chemicals and Loba Chemicals. Every chemical was used exactly as it was delivered.

2.2. Softwares and Databases required

ACD/ChemSketch downloaded from www.acdlabs.com (create and modify images of chemical structures); Lipinski drug-likeness evaluation performed using molinspiration server; SwissADME accessed through the Swiss Institute of Bioinformatics web server; pkCSM (ADMET prediction); ProTox-3.0 accessed via the online toxicity prediction server; Protein Data Bank (PDB) structures retrieved from www.rcsb.org; BIOVIA Discovery Studio Visualizer downloaded from www.accelrys.com (examining, exchanging, and evaluating data on proteins and tiny molecules); PyRx downloaded from pyrx.sourceforge.net (Estimate the binding energy of ligands to receptors).

2.3. Lipinski's five rules

The frameworks made with Chems sketch software were first examined for Lipinski's rule of 5 using the Molinspiration software. Regarding the frameworks which have been sketched and entered into the designated tab of the online SMILES translator, the SMILES notation was created. The properties were computed after choosing the "Calculate of molecular properties and bioactivity prediction" option.^[17]

2.4. ADMET properties

The ADMET score of the scaffolds was examined using the pkCSM prediction tool by submitting their SMILES representations to estimate absorption, distribution, metabolism, excretion, and toxicity characteristics. Hepatotoxicity, CYP2D6 inhibition, BBB penetration, and HIA are among the ADMET characteristics that were computed. PyRx was used to do molecular docking experiments on chalcone hybrids that had passed the Lipinski's rule of 5 and ADMET analysis.

2.5. Docking studies

2.5.1. Protein preparation

The RCSB Protein Data Bank (PDB) provided the target protein's 3D structure. Polar hydrogens were introduced, water molecules and unnecessary heteroatoms were eliminated, and the structure had been converted to PDBQT format using AutoDock Tools integrated within PyRx.^[18]

2.5.2. Ligand preparation

Ligand structures were drawn using ChemDraw and converted to SMILES format. The ligands were imported into PyRx and minimized their energy utilising the Universal Force Field (UFF), and saved in PDBQT file for docking.^[19]

2.5.3. Grid box definition

A grid box was defined to encompass the protein's active site and specify the docking search space. The center coordinates and dimensions of the box were adjusted to cover the binding pocket effectively.^[20]

2.5.4. Docking simulations

In PyRx, docking was done with the AutoDock Vina engine, generating multiple conformations of each ligand and calculating binding affinities based on the scoring function.^[20]

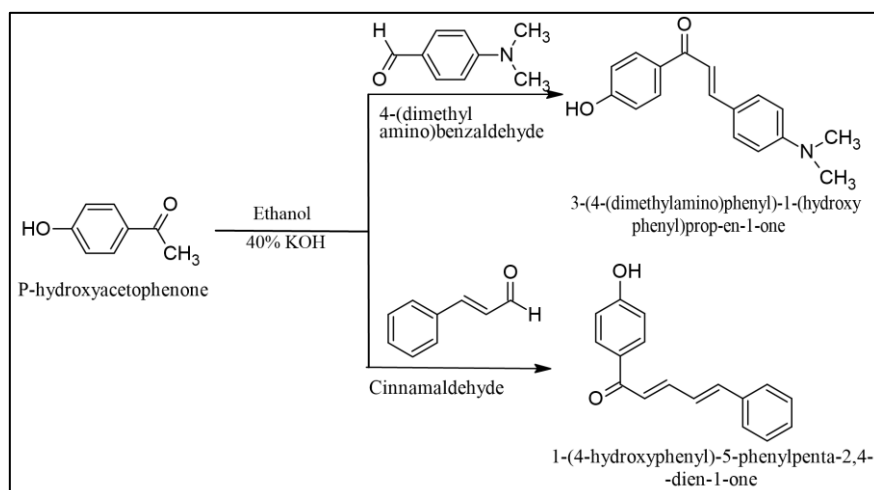
2.5.5. Analysis of docked complexes

The best-scoring conformation was chosen for study after the docked poses were ordered based on binding energy. Discovery Studio was used to show protein–ligand interactions, including π - π , hydrophobic, and hydrogen bonding interactions.^[21]

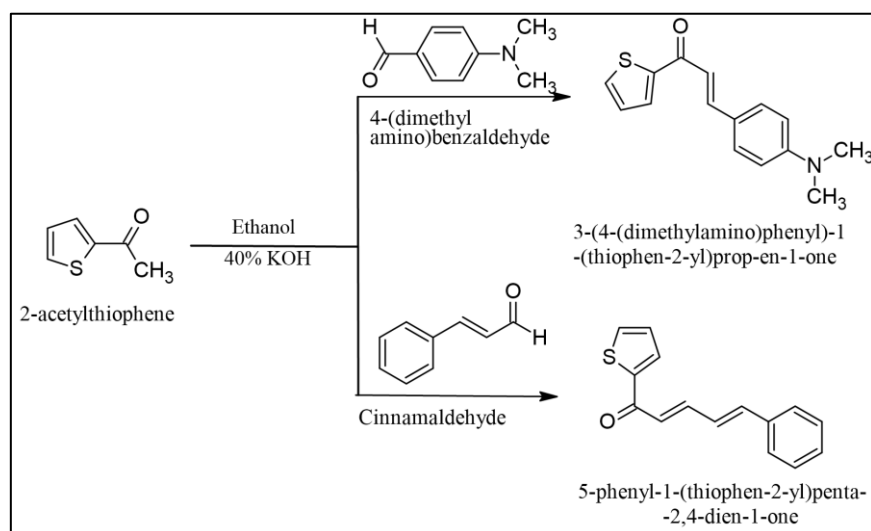
2.4. Experimental Section

2.4.1. Synthesis

Aryl and heteroaryl chalcone hybrids were prepared using the Claisen–Schmidt condensation method. After dissolving equivalent quantities of aromatic aldehyde and substituted acetophenone in ethanol, one or two drops of aqueous NaOH were added as a catalyst. For several hours, the reaction mixture was agitated at room temperature while thin-layer chromatography (TLC) was being used for monitoring. Filtration, cold ethanol cleaning, and recrystallization were used to obtain pure chalcone derivatives as given in **scheme 1** and **scheme 2**.^[22]



Scheme 1: Preparation of aryl chalcone derivatives.



Scheme 2: Preparation of heteroaryl chalcone derivatives.

3. RESULTS AND DISCUSSION

3.1. Lipinski's five rules and ADMET analysis

Poor pharmacokinetics and toxicity are the main causes of medication failures. Compounds were screened using ADMET analysis and Lipinski's rule of 5 in order to reduce this. Although Lipinski's rule permits up to two violations and predicts oral bioavailability based on molecular weight under 500D, log P under 5, HBD under 5, and HBA under 10, it does not reveal pharmacological activity. [23-25]

Online software called pkCSM was used to determine the ADMET property of the designed derivatives. The program forecasts the inhibitors of p-glycoproteins 1 and 2, intestinal absorption, skin permeability, calcium carbonate permeability, and water solubility. The program forecasts the following: toxicity (Hepatotoxicity, Carcinogenicity, Immunotoxicity, Mutagenicity, cytotoxicity), excretion (total clearance and renal clearance OCT2 substrate), metabolism (CYP2D6 substrate, CYP3A4 substrate, CYP3A4 inhibitor, CYP1A2 inhibitor, CYP2C9 inhibitor, CYP2D6 inhibitor, CYP3A4 inhibitor), distribution (VDss human), fraction unbound, BBB permeability, and CNS permeability.

These findings in the current study can be used to build new medications because all of the proposed derivatives' ADME parameters are within the acceptable range for humans. **Tables 1 and 2** provide an overview of the chosen compounds that satisfy Lipinski's requirements and advantageous ADMET values.

Table No. 1: Lipinski's rule of 5 of the synthesized compounds.

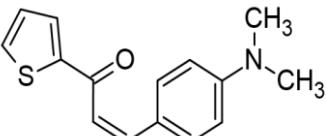
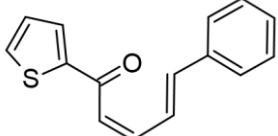
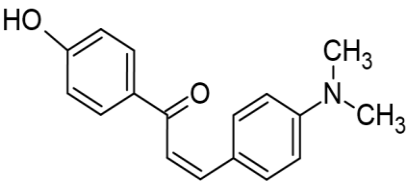
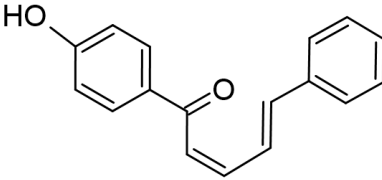
Code	Structure	MW (g)	Log P	HBA	HBD	NRotB
ATP ₁		257.35	3.39	1	0	4
ATP ₂		240.32	3.88	1	0	4
ACP ₁		267.32	3.05	2	1	4
ACP ₂		250.29	4.26	1	0	4



Table No. 2: ADMET/TOX profiles of the designed compounds.

Prop.	Molecular descriptions	ATP ₁	ATP ₂	ACP ₁	ACP ₂	STD
A	Water solubility (log mol/l)	-4.87	-4.899	-4.285	-4.471	-1.504
	CaCO ₂ permeability (log Papp)	1.192	1.861	1.446	1.597	0.582
	Intestinal absorption (%)	94.783	94.038	94.789	93.014	92.111
	Permeability of skin (log kp)	-2.137	-2.1	-2.536	-2.518	-3.564
	Substrate for p-glycoprotein	N	N	Y	Y	N
	Inhibitor for P-glycoprotein 1 & 2	N	N	N	N	N
D	VDss(Human) (log L/kg)	0.373	0.529	0.369	0.302	-0.405
	Fraction unbound (Fu)	0.003	0	0.114	0.055	0.757
	BBB permeability (log BB)	0.429	0.546	0.081	0.081	-0.432
	CNS permeability (log PS)	-1.375	-1.266	-1.442	-1.353	-3.43
M	Substrate for CYP2D6	N	N	N	N	N
	Substrate for CYP3A4	Y	Y	N	N	N
	Inhibitor for CYP1A2	Y	Y	Y	Y	N
	Inhibitor for CYP2C19	Y	Y	Y	Y	N
	Inhibitor for CYP2C9	Y	Y	Y	Y	N
	Inhibitor for CYP2D6	N	N	N	N	N
	Inhibitor for CYP3A4	N	N	N	N	N
E	Total clearance (log ml/min/kg)	0.128	0.16	0.331	0.16	0.642
	Substrate of Renal OCT2	N	N	N	N	N
T	Predicted Ld50(mg/kg)	1800	1800	3000	1048	1923
	Predicted toxicity class	4	4	5	4	4
	TPSA	48.55	37.3	40.54	37.3	65.27
	Hepatotoxicity	-	-	-	-	-
	Carcinogenicity	-	-	-	-	+
	Immunotoxicity	-	-	+	-	-
	Mutagenicity	-	-	-	-	-
	cytotoxicity	-	-	-	-	-

3.2. Molecular Docking

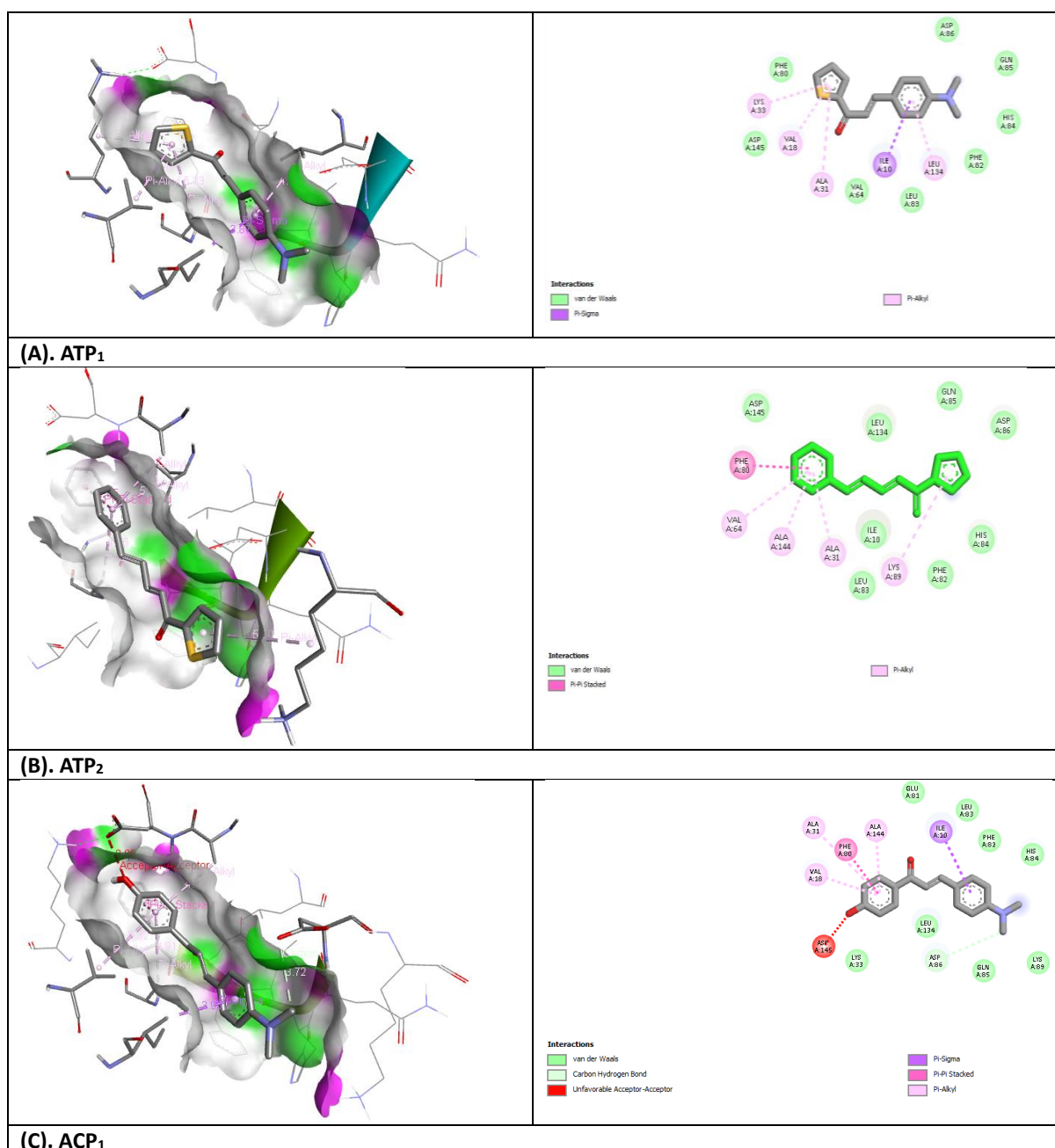
Molecular docking experiments aid in identifying potential interactions between the CDK2 enzyme and chalcone derivatives. It was discovered that the created compounds have a high affinity for binding to the enzyme. The chosen compounds' binding affinities, which ranged from -6.3 to -8.5 kcal/mol, demonstrated that they may have CDK2 enzyme inhibitory binding sites. (Table 3). According to the PyRx data, ATP₁ has an energy of -8.5 Kcal/mol when the 2FVD inhibitor interacts with the intended molecules for the anticancer activity. ACP₁ has an energy of -7.1 Kcal/mol when the 1MWT inhibitor interacts with the intended molecules for antimicrobial activity. ACP₂ has an energy of -8.1 Kcal/mol when the 4JK4 inhibitor interacts with the intended molecules for antioxidant activity. ATP₂ has an energy of -7.4 Kcal/mol when the 4O2B inhibitor interacts with the intended molecules for anthelmintic activity.

Table No. 3: Binding energies (Kcal/mol) of the aryl and heteroaryl chalcone hybrids.

Code	Anticancer activity PDB ID: 2FVD	Antimicrobial activity PDB ID: 1MWT	Antioxidant activity PDB ID: 4JK4	Anthelmintic activity PDB ID: 4O2B
ATP ₁	-8.5	-6.9	-8.0	-7.2
ATP ₂	-8.2	-6.5	-8.0	-7.4
ACP ₁	-7.9	-7.1	-7.7	-6.8
ACP ₂	-7.4	-6.3	-8.1	-6.4
5-FLUOROURACIL	-7.7	---	---	---
GENTAMICIN	---	-7.1	---	---
ASCORBIC ACID	----	---	-7.8	---
ALBENDAZOLE	---	---	---	-7.0

3.2.1. Molecular docking interactions with PDB ID 2FVD

Figure 2 shows a number of interactions between the docked conformation of 2FVD and the active conformation of chalcone hybrids A-D. ATP₁ Showed van der waals interaction with PHE80, ASP145, VAL64, LEU83, PHE82, HIS84, GLN85 and ASP86. It shows pi-sigma interactions with ILE10 and pi-alkyl interactions with LYS33, VAL18, ALA31, LEU134. It was discovered that the binding strength was -8.5 Kcal/mol. ATP₂ showed Van der waals interaction with ASP145, ILE10, LEU83, PHE82, HIS84, LEU134, GLN85, ASP86. It shows pi-pi bonding with PHE80 and pi-alkyl bonding with VAL64, ALA144, ALA31 and LYS89. It was discovered that the binding strength was -8.2 Kcal/mol. ACP₁ forms one carbon hydrogen bond with ASP86; van der waals interaction with GLU81, LEU83, PHE82, HIS84, LYS89, GLN85, LEU134, LYS33; pi-sigma interaction with ILE10; pi-pi stacking with PHE80; pi-alkyl interaction with ALA144, ALA31, VAL18 and unfavorable acceptor-acceptor with ASP145. It was discovered that the binding strength was -7.9 Kcal/mol. ACP₂ showed van der waals interaction with PHE82, HIS84, LEU83, LEU134, VAL64, GLU81, LYS 33; pi-pi stacking with PHE80; pi-alkyl bonding with ILE10, ALA31, VAL18, ALA144; and unfavorable acceptor-acceptor interaction with ASP145. It was discovered that the binding strength was -7.4 Kcal/mol. ATP₁ showed the highest binding strength and can be used for anticancer studies.



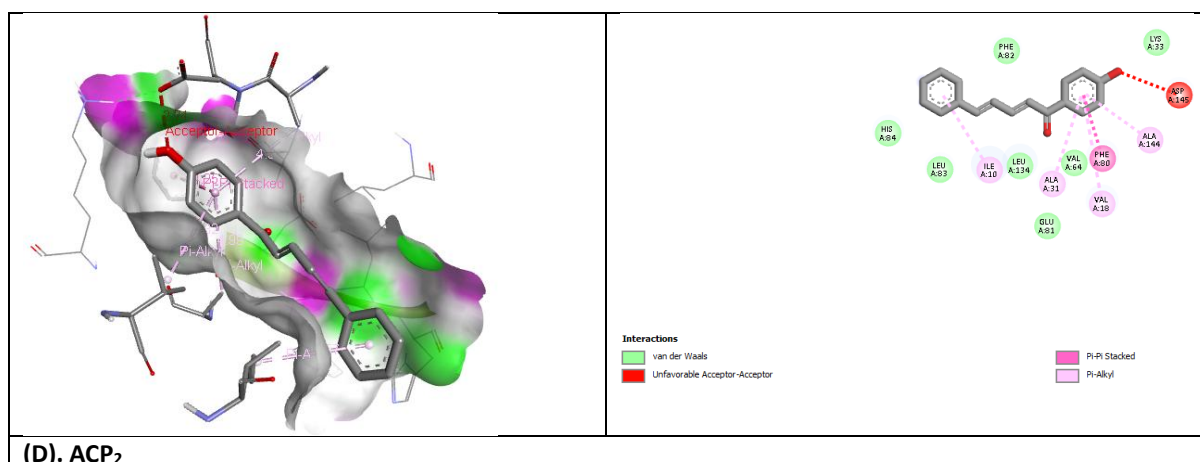
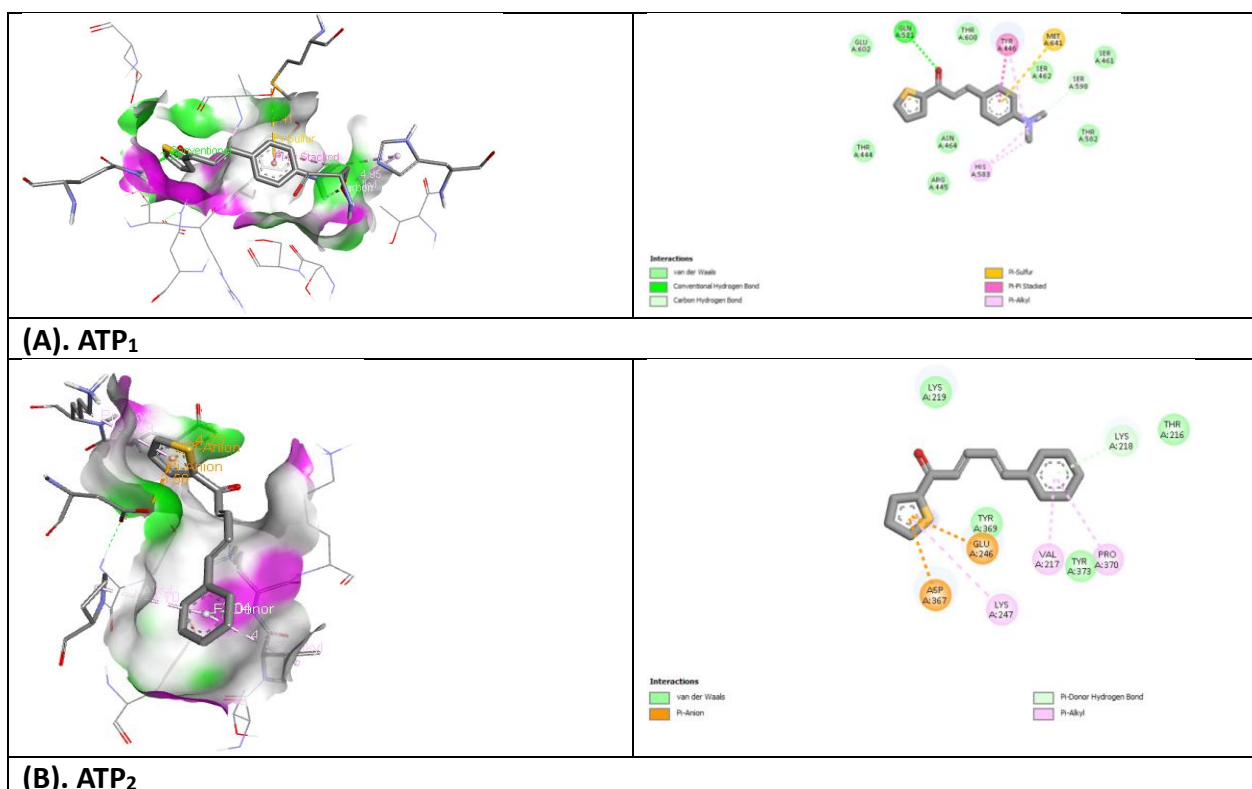


Fig. 2: shows the docking visualization between PDB ID 2FVD and (A)-(D)

3.2.2. Molecular docking interactions with PDB ID 1MWT

Figure 3 shows a number of interactions between the docked conformation of 1MWT and the active conformation of chalcone hybrids A-D. ATP₁ showed conventional hydrogen bonding with GLN521 and carbon hydrogen bond with SER598. It also showed van der Waals interaction with THR444, GLU602, THR600, ASA464, THR 582, SER462 AND SER 461. It shows pi-sulfur interactions with MET641; pi-pi stacking with TYR446 and pi-alkyl bonding with HIS583. It was discovered that the binding strength was -6.9 Kcal/mol. ATP₂ showed van der Waals interaction with LYS219, TYR369, TYR373 AND THR216. It shows pi-anion bonding with ASP367 and GLU246; pi-donor hydrogen bonding with LYS218; and pi-alkyl bonding with LYS247, VAL217, PRO370. It was discovered that the binding strength was -6.5 Kcal/mol. ACP₁ forms conventional hydrogen bonding with LYS406 and SER462. It showed van der Waals interaction with HIS583, SER598, GLY599, THR600, SER403, ASN464, TYR446 and LYS430; and pi-alkyl bonding with ALA642. It was discovered that the binding strength was -7.1 Kcal/mol. ACP₂ forms conventional hydrogen bonding with HIS251, LYS285 and ASN393. It showed van der Waals interaction with GLY282, LEU252, TYR496, GLN396, GLU268 and LYS289; and pi-alkyl bonding with LYS281 and LEU286. It was discovered that the binding strength was -6.3 Kcal/mol. ACP₁ showed the highest binding strength and can be used for antimicrobial studies.



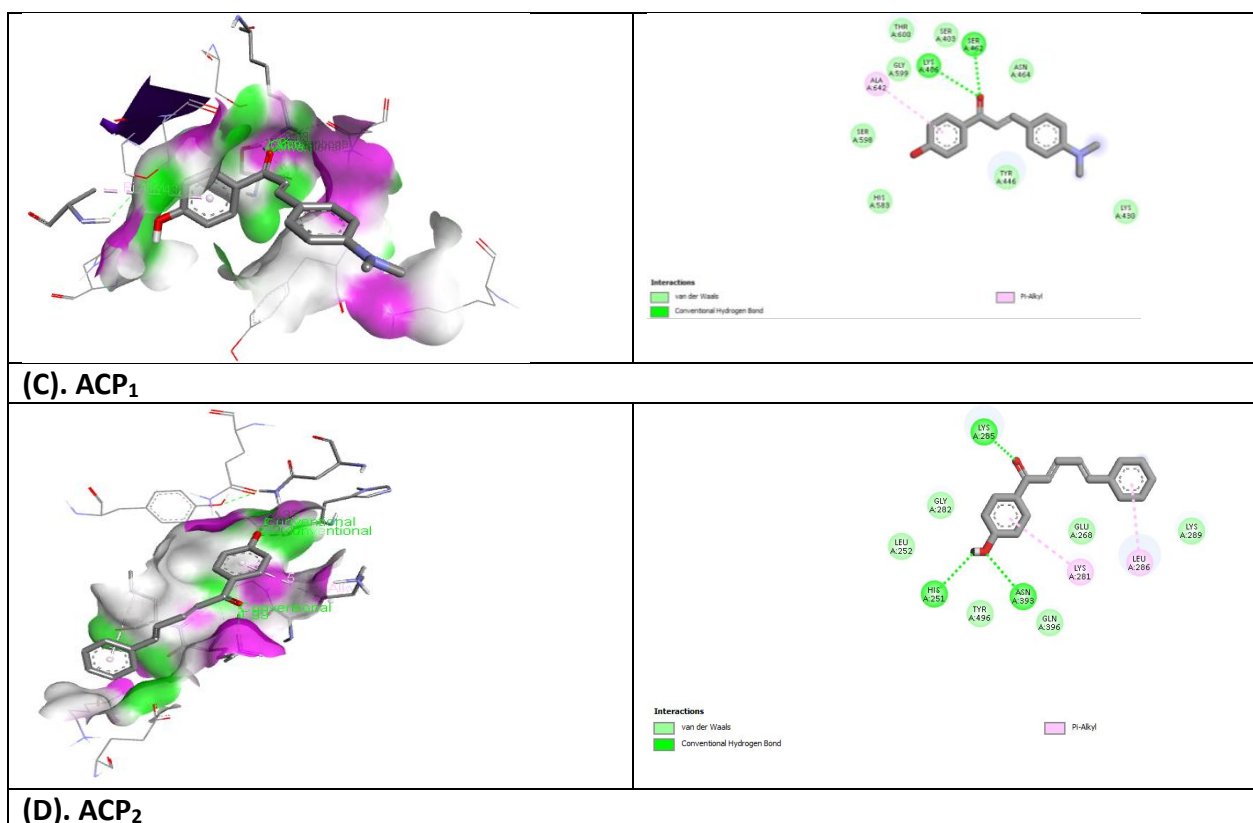
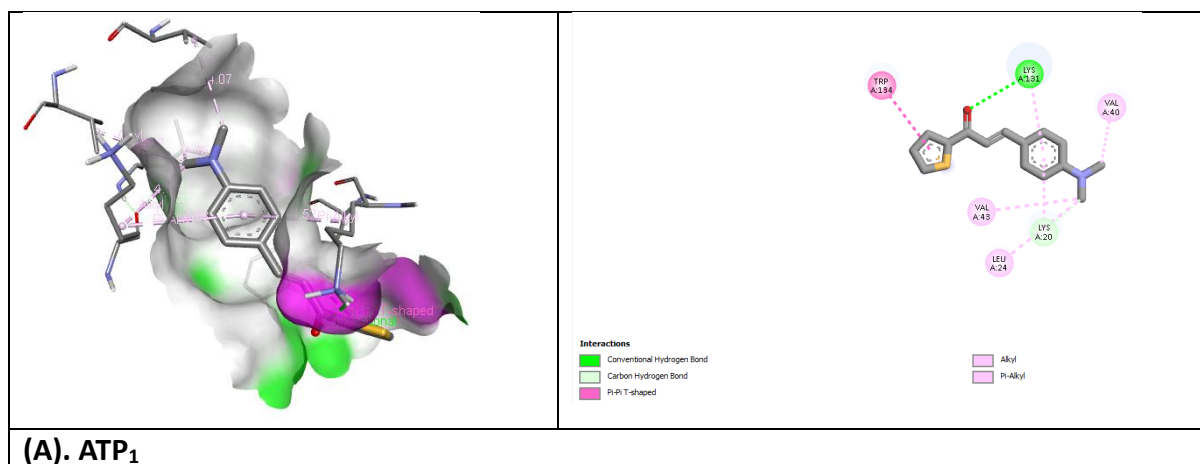


Fig. 3: shows the docking visualization between PDB ID 1MWT and (A)-(D)

3.2.3. Molecular docking interactions with PDB ID 4JK4

Figure 4 shows a number of interactions between the docked conformation of 4JKA and the active conformation of chalcone hybrids A-D. ATP₁ forms one conventional hydrogen bonding with LYS131 and one carbon hydrogen bonding with LYS20. It shows pi-pi T shaped interaction with TRP134 and pi-alkyl bonding with VAL43, LEU24 and VAL40. It was discovered that the binding strength was -8.0 Kcal/mol. ATP₂ forms two conventional hydrogen bonding with THR305 and LEU304; and pi-alkyl bonding with ARG336. It was discovered that the binding strength was -8.0 Kcal/mol. ACP₁ forms one conventional hydrogen bonding with ASP323 and carbon hydrogen bond with PHE205. It showed van der waals interaction with GLY327, LEU330, ALA349, LEU346, LEU480, GLU478 and ARG208; pi-cation interaction with LYS350; and pi-alkyl interaction with LEU326 and ALA212. It was discovered that the binding strength was -7.7 Kcal/mol. ACP₂ forms three conventional hydrogen bonding with THR305, LEU304 and PHE373. It showed van der waals interaction with LEU301, PRO303, TYR333 and LYS377; pi-pi T shaped interaction with HIS337; and pi-alkyl bonding with ARG336. It was discovered that the binding strength was -8.1 Kcal/mol. ACP₂ showed the highest binding strength and can be used for antioxidant studies.



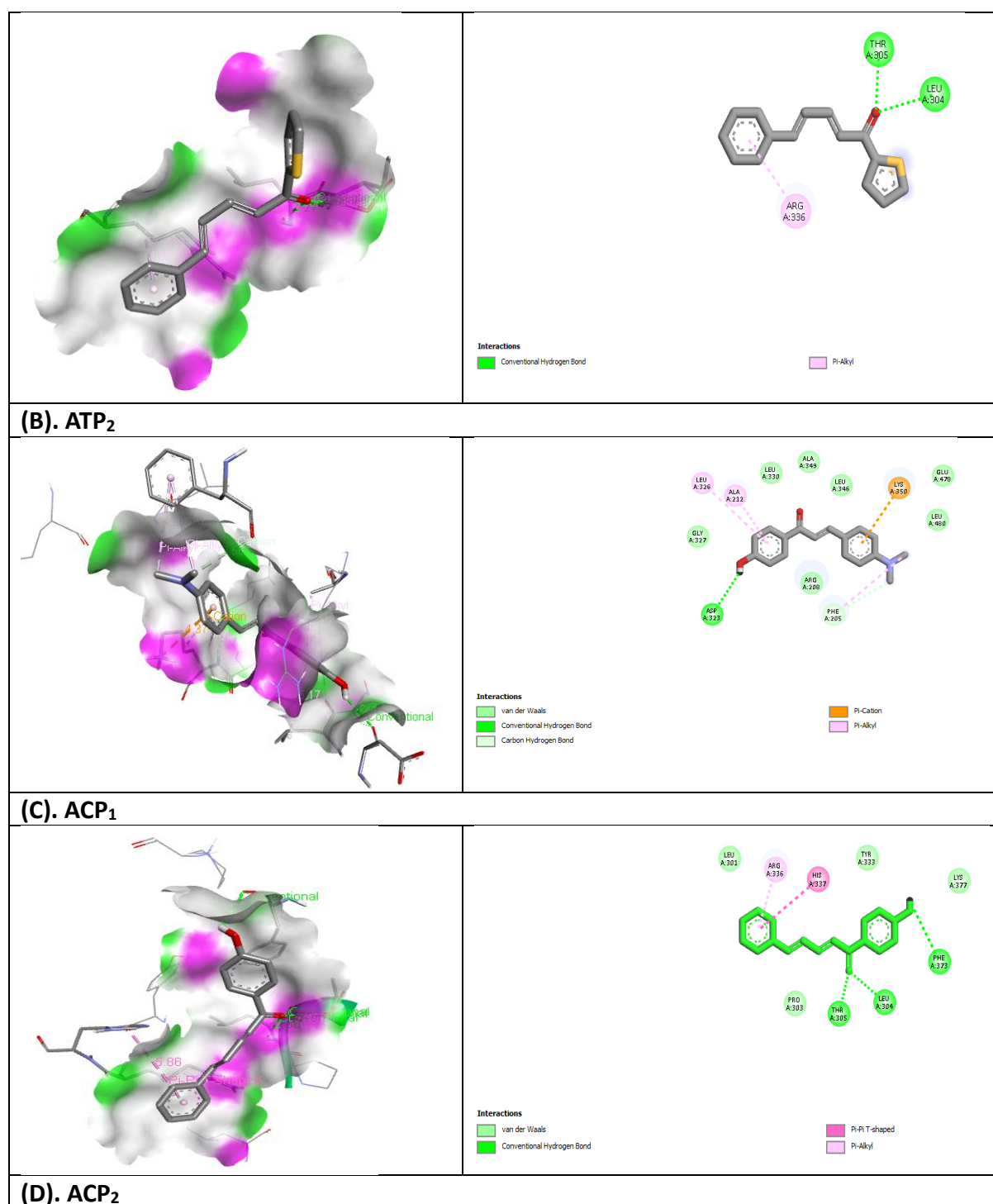


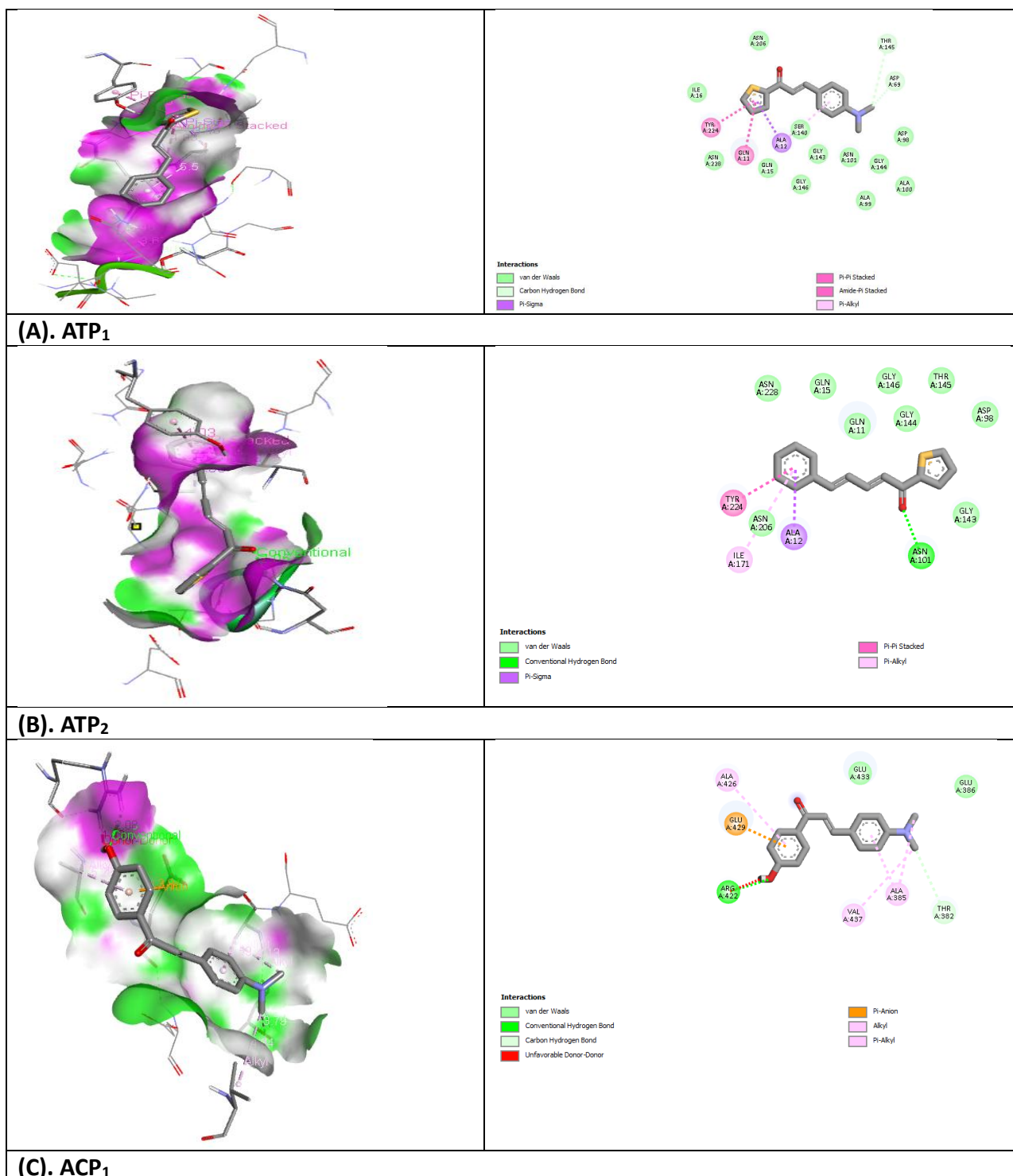
Fig. 4: shows the docking visualization between PDB ID 4JK4 and (A)-(D)

3.2.4. Molecular docking interactions with PDB ID 4O2B

Figure 5 shows a number of interactions between the docked conformation of 4O2B and the active conformation of chalcone hybrids A-D. ATP₁ showed two carbon hydrogen bonding with THR145 and ASP69. It also showed van der Waals interaction with ASN206, ILE16, ASN228, GLN15, GLY146, SER140, GLY143, ASN101, GLY144, ALA99, ALA100 and ASP98. It shows pi-sigma interactions with ALA12; pi-pi stacking with TYR224; amide-pi stacking with GLN11; and pi-alkyl bonding with ALA12. It was discovered that the binding strength was -7.2 Kcal/mol. ATP₂ forms one conventional hydrogen bond with ASN101; showed van der Waals interaction with ASN228, GLN15, GLN11, GLY144, GLY146, THR145, ASP98, GLY143, and ASN206; pi-sigma

interactions with ALA12; pi-pi stacking with TYR224; and pi-alkyl bonding with ILE171. It was discovered that the binding strength was -7.4 Kcal/mol.

ACP₁ forms one conventional hydrogen bonding with ARG422 and one carbon hydrogen bonding with THR382. It showed van der waals interaction with GLU433 and GLU386; pi-alkyl bonding with ALA426, VAL437 and ALA385; and pi-anion interaction with GLU429. It was discovered that the binding strength was -6.8 Kcal/mol. ACP₂ forms one conventional hydrogen bonding with THR82 and one carbon hydrogen bonding with GLY81. It showed van der waals interaction with GLU77, TYR83, GLU22, TRP21, PHE87, ASN18, THR225, ASN228, TYR224 and GLN15; and pi-alkyl bonding with VAL78. It was discovered that the binding strength was -6.4 Kcal/mol. ATP₂ showed the highest binding strength and can be used for anthelmintic studies.



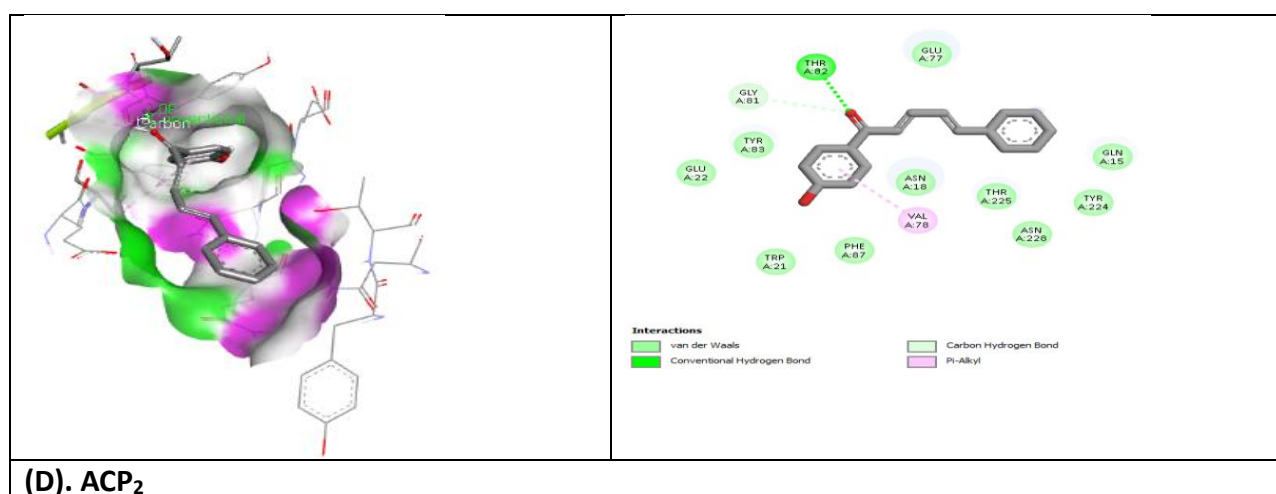


Fig. 5: shows the docking visualization between PDB ID 4O2B and (A)-(D)

4. CONCLUSION

This study's thorough in silico evaluation effectively illustrated the potential of novel aryl and heteroaryl chalcone derivatives as prospective CDK2 inhibitors. Molecular docking studies against CDK2 proteins revealed favorable binding affinities and significant interactions with key active site residues, indicating strong inhibitory potential. ADMET and drug-likeness predictions confirmed acceptable pharmacokinetic properties and low toxicity risks for most of the designed compounds. Protein validation studies further supported the reliability of the docking results. Overall, the findings suggest that these chalcone derivatives could be used as lead molecules to create novel anticancer drugs targeting CDK2. To confirm their biological effectiveness and therapeutic potential, more in vitro and in vivo research is necessary.

5. ACKNOWLEDGEMENT

We are deeply grateful to the management of Grace College of Pharmacy, Kodunthirappully, Palakkad, Kerala for giving us the encouragement, resources, and assistance we needed to finish this project. Their leadership and dedication to academic success have been crucial to our success.

6. REFERENCES

- [1] Malumbres M, Barbacid M. Cell cycle, CDKs and cancer: a changing paradigm. *Nat Rev Cancer*. 2009;9(3):153–166.
- [2] Morgan DO. Cyclin-dependent kinases: engines, clocks, and microprocessors. *Annu Rev Cell Dev Biol*. 1997; 13:261–291.
- [3] Tadesse S, Yu M, Kumarasiri M, et al. Targeting CDK2 in cancer: challenges and opportunities. *Cancer Lett*. 2015;364(2):133–141.
- [4] Asghar U, Witkiewicz AK, Turner NC, Knudsen ES. The history and future of targeting cyclin-dependent kinases in cancer therapy. *Nat Rev Drug Discov*. 2015;14(2):130–146.
- [5] Otto T, Sicinski P. Cell cycle proteins as promising targets in cancer therapy. *Nat Rev Cancer*. 2017;17(2):93–115. Whittaker SR, Mallinger A, Workman P, Clarke PA. Inhibitors of cyclin-dependent kinases as cancer therapeutics. *Pharmacol Ther*. 2017; 173:83–105.
- [6] Senderowicz AM. Cyclin-dependent kinase inhibitors: past successes and future challenges. *Oncogene*. 2003;22(43):6609–6620.
- [7] Fischer PM. CDK inhibitors: a patent review (2010–2015). *Expert Opin Ther Pat*. 2017;27(2):159–168.
- [8] Nowakowska Z. A review of anti-infective and anti-inflammatory chalcones. *Eur J Med Chem*. 2007;42(2):125–137.
- [9] Batovska DI, Todorova IT. Trends in utilization of the pharmacological potential of chalcones. *Curr Clin Pharmacol*. 2010;5(1):1–29.
- [10] Zhuang C, Zhang W, Sheng C, et al. Chalcone: a privileged structure in medicinal chemistry. *Chem Rev*. 2017;117(12):7762–7810.
- [11] Kumar D, Jain SK. Chalcone derivatives as potential anticancer agents: a review. *Mini Rev Med Chem*. 2016;16(12):935–958.
- [12] Abdel-Aziz HA, Eldehna WM, Keeton AB, Piazza GA. Design and synthesis of novel chalcone derivatives as potential anticancer agents. *Eur J Med Chem*. 2014; 70:358–363.



- [13] Eldehna WM, Fares M, Abdel-Aziz MM, et al. Synthesis and biological evaluation of certain chalcone-based CDK inhibitors. *Bioorg Chem.* 2018; 76:332–342.
- [14] Lionta E, Spyrou G, Vassilatis DK, Cournia Z. Structure-based virtual screening for drug discovery: principles, applications and recent advances. *Curr Top Med Chem.* 2014;14(16):1923–1938.
- [15] van de Waterbeemd H, Gifford E. ADMET in silico modelling: towards prediction paradise. *Nat Rev Drug Discov.* 2003;2(3):192–204.
- [16] Ferreira LG, dos Santos RN, Oliva G, Andricopulo AD. Molecular docking and structure-based drug design strategies. *Molecules.* 2015;20(7):13384–13421.
- [17] Asokkumar K, Prathyusha LT, Umamaheshwari M, Sivashanmugam T, Subhadradevi V, Jagannath P, et al. Design, ADMET and docking studies on some novel chalcone derivatives as soluble epoxide hydrolase enzyme inhibitors. *J Chil Chem Soc.* 2012;57(4):1442.
- [18] Morris GM, Huey R, Lindstrom W, et al. AutoDock4 and AutoDockTools4: automated docking with selective receptor flexibility. *J Comput Chem.* 2009;30(16):2785–2791.
- [19] Dallakyan S, Olson AJ. Small-molecule library screening by docking with PyRx. *Methods Mol Biol.* 2015; 1263:243–250.
- [20] Trott O, Olson AJ. AutoDock Vina: improving the speed and accuracy of docking with a new scoring function, efficient optimization, and multithreading. *J Comput Chem.* 2010;31(2):455–461.
- [21] Goodsell DS, Morris GM, Olson AJ. Automated docking of flexible ligands: applications of AutoDock. *J Mol Recognit.* 1996;9(1):1-5.
- [22] Patel D, Patel M, Parmar P, et al. Synthesis and biological evaluation of chalcone derivatives as antimicrobial agents. *Int J ChemTech Res.* 2013;5(2):587–592.
- [23] S. Ekins, Y. Nikolsky, T. Nikolskaya, *Trends Pharmacol. Sci.* 26, 202(2005).
- [24] W.J. Egan, G. Zlokarnik, P.D.J. Grootenhuis, *Drug Dis.Today Tech.* 1, 381(2004).
- [25] C.A. Lipinski, F. Lombardo, B.W. Dominy, P.J. Feeney, *Adv. Drug Del. Rev.* 46, 3 (2001).

How to cite this article:

Priyanka S et al. *Ijppr.Human*, 2026; Vol. 32 (2): 261-272.

Conflict of Interest Statement: All authors have nothing else to disclose.

This is an open access article under the terms of the Creative Commons Attribution-NonCommercial-NoDerivs License, which permits use and distribution in any medium, provided the original work is properly cited, the use is non-commercial and no modifications or adaptations are made.